DETERMINATION OF THE BEAGLE2 LANDING SITE

R. Trautner [(1)], N. Manaud [(2)], G. Michael [(1)], A. Griffiths[(3)],
S. Beauvivre[(4)], D. Koschny [(1)], A. Coates[(3)], J-L. Josset[(4)]

[1] *Research and Scientific Support Department, ESA/ESTEC, 2200 AG Noordwijk, The Netherlands*
[2] *Institut d'Astrophysique Spatiale, Université Paris-Sud, F-91405 Orsay, France*
[3] *Mullard Space Science Laboratory, University College London, Holmbury St. Mary, Dorking, RH5 6NT, UK*
[4] *SPACE-X, Jaquet-Droz 1, CH-2007 Neuchâtel, Switzerland*

Roland.Trautner@esa.int   Tel: +31 71 565 3955   Fax: +31 71 565 4697

ABSTRACT

Beagle2 is the UK-led lander element on ESA's Mars Express mission, which will reach Mars in late December 2003. After separation from the Mars Express orbiter 6 days before the atmospheric entry, Beagle2 will descend to the Martian surface by means of ablative heat shields and parachutes. The impact will be cushioned by a set of airbags.

The selected landing site at 11.6 deg N / 90.75 deg E (IAU 2000 coordinates) is situated in the south-east of the center of Isidis Planitia, a sedimentary basin which is expected to meet the requirements of Beagle's scientific mission, the lander operations, and the entry, descent and landing systems. The exact determination of the Beagle2 landing site is important not only for the Beagle2 and MEX orbiter science investigations, but also for the reconstruction of Beagle's entry and descent trajectory.

A precise determination of the Beagle2 position is not possible via the MELACOM radio link. Instead, a novel method based on celestial navigation is employed, which utilizes the Stereo Camera System on the lander for imaging the Martian night sky. The position data is then refined by comparing the landing site panorama images with high resolution orbiter images and laser altimeter data. This combination of celestial navigation with image data analysis for precision position determination will be applicable for many future missions as well.

1. INTRODUCTION

The precise determination of the position of a scientific planetary lander after its touchdown is an important issue for a number of reasons. For the science investigations, it is important to know the scientific context of the landing site. The coordination of science operations with an orbiter depends on the correct and timely identification of the lander location. From an engineering perspective, the knowledge of the final position is important for the reconstruction of the entry, descent and landing trajectory. For accurate planning of communications and power budgets the lander attitude plays an important role. Ideally, the position of a lander should be known as soon as possible after its touchdown in order to allow a reliable assessment of its status, and for being able to safely plan its surface operations.

Previous Mars missions have relied predominantly on position determination via a direct lander-earth radio link. For the Viking 1 lander, the search area for its detailed location on Mars was determined by the Viking lander radio science team via Doppler tracking. In a second step, the correlation of topographic features seen on lander panorama images with features identified in orbiter images was used in order to obtain the position of the lander [1]. Later on this result was improved using the same technique but higher resolution orbiter imagery [2]. A different landing site was suggested after a recalculation of the Viking Mars control point network [3]. More recent work proposes another alternative landing site [4].

For the Viking 2 lander, the operations teams attempted to determine the position in a similar manner. However, due to the lack of prominent horizon features in the lander's neighbourhood its position was not undisputedly established [5]. Recent work on the panoramic images using improved image processing techniques could not resolve the ambiguity in the position results [6],[7]. In the case of Mars Pathfinder, the identification of the landing site was comparatively straightforward due to the abundance of many prominent features on the horizon [7]. Again the location was determined by using radio tracking data for restricting the search area, and orbiter images together with lander panoramas.

For the European Beagle2 lander, all communications will rely on the Mars Express and Mars Odyssey orbiters. Furthermore, the transceivers on the orbiters do not support accurate Doppler measurements on the communications link. Therefore a position determination via the radio link is not possible. Instead, the search area for the comparison of lander panoramas

and high resolution orbiter images will be determined using celestial navigation.

In the following sections, the SCS camera system and the navigation methods employed for Beagle2 will be described. The lander location accuracy and implementation strategy will be presented, and possible future applications will be briefly discussed.

2. THE BEAGLE2 STEREO CAMERA SYSTEM

The Stereo Camera System (SCS) provides the primary imaging capability of the Beagle 2 Mars lander [8]. Sensitive to visible and near IR wavelengths (440–1000 nm), it consists of twin camera/filter wheel units, or "eyes". One "eye" is composed of a highly integrated micro-camera incorporating a frame transfer CCD array of 1024x1024 pixels and all the electronics (sequencer, converter, internal buffer for up to 4 images, internal clock) to realise a complete camera delivering a 10 bits digital output at 10 Mbits/s. [9]. The wide-angle optics (48° field of view per "eye") and a choice of 24 filters allow a wide range of scientific objectives to be addressed. Some basic performance figures and optical parameters are shown in Table 1. The titanium filter wheel is enclosed by an aluminium housing and lid (with radiation hard BK7 optical window) and is driven by a stepper motor and gear wheel assembly. A stainless steel wiper blade attached to the central gear shaft is provided to remove dust from the optical window. The Stereo Cameras are mounted on the position adjustable workbench, or PAW (stereo baseline = 209 mm and toe-in = 3.73° per "eye") at the end of the 0.7 m long robot arm.

Once an image has been acquired, it is transmitted to the spacecraft and compressed by the lander software using a lossy wavelet-encoding scheme [10]. The circular illumination pattern of the 48° optics selected for Beagle2 does not completely overlap the CCD, leaving the corners unilluminated. Due to the depth of focus available with the camera optics, two working distances are required: The 48° optics are optimised for viewing high priority objects within reach of the lander's robot arm (i.e. best focus between 0.6 and 1.2 m). To view objects at greater distances four lenticular filters are used. For celestial images, these filters offer the best sensitivity. Measured values of system gain are 792 ± 21 electrons/DN for the left eye and 663 ± 16 electrons/DN for the right. The manufacturer's quantum efficiency curve peaks at ~20% and combined with the equation 1 of [11], yields a preliminary responsivity of ~65 DN/s per W/(m^2 st µm) for the left #8 filter (centre wavelength = 670 nm). This will be the main filter used for the acquisition of celestial images for navigation purposes. The sensitivity of the SCS system for imaging celestial navigation targets was demonstrated in a dedicated test campaign.

Table 1. Stereo Camera System optical characteristics

Parameter	Value
Focal length	
-Lenticular filters	22.71 mm
-Flat filters	22.26 mm
Toe-in angle	3.73°
Stereo Baseline	209 mm
Field of View	48.0° (manufacturer)
(each Camera)	41.8° (illuminated [b])
FOV 100% Overlap	
Distance	1.2 m
Minimum focusing distance[a]	
-Flat filters	0.6 m
-Lenticular Filters	1.2 m
Maximum focusing distance[a]	
-Flat filters	1.2 m
-Lenticular Filters	infinity
Scale	0.75 mrad / pixel
Exposure time	1–65535 ms
Frame transfer	1 ms
Readout time	1132 ms
Spectral range	440–1000 nm
A/D Conversion	10 bits / pixel
Read out noise [electrons]	292 ± 26 Left 257 ± 22 Right
Full well [electrons]	$811 \pm 0.90 \times 10^3$ Left $679 \pm 0.82 \times 10^3$ Right
Gain [electrons/DN][c]	792 ± 21 Left 663 ± 16 Right
Signal to Noise Ratio[d]	857 Left 786 Right
Number of Pixels	1024 x 1024
Pixel Size	14 x 14 µm

[a] For sharp focus over entire field of view.
[b] Measured during calibration campaign.
[c] Values under revision
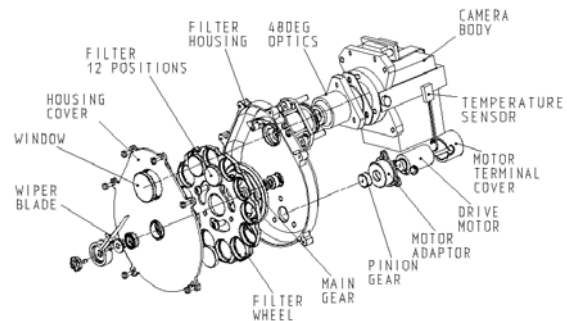[d] i.e. Full well divided by the quadrature of shot and readout noise

Fig. 1. The Beagle2 Stereo Camera System

3. CELESTIAL NAVIGATION FOR BEAGLE2

The celestial navigation method employed for Beagle2 relies on celestial objects populating orbits that are relatively close to the lander. In the case of Mars, there are two natural targets that fulfil this requirement – Phobos and Deimos. Their basic properties are shown in Table 2 [12].

Table 2. Phobos and Deimos properties

	Phobos	Deimos
Major axes	26x18 km	16x10 km
Orbital velocity	2.14 km/sec	1.35 km/sec
Distance	9377 km	23436 km

When an image of such an object (called 'navigation target body' in the following text) together with the star background is taken from the lander position, the separation angle between the photometric center of a star and the target body can be calculated. A model of the body and the illumination phase angle will allow determination of the offset between the photometric center and the center of gravity (COG), and thus the separation angle α between the star and the COG of the target as seen from the landing site. For any particular orbiting navigation target and unique point in time, a cone with inner angle α can be constructed, which originates at the COG of the navigation target, and intersects with the surface of the lander target body (which is Mars in the case of Beagle2). The intersection represents all points on the surface of the lander target body, from where the orbiting object can be seen under the observed separation angle at the time when the image has been taken. Fig. 2 illustrates this principle, with Mars as the lander target body, and Phobos as the navigation target.
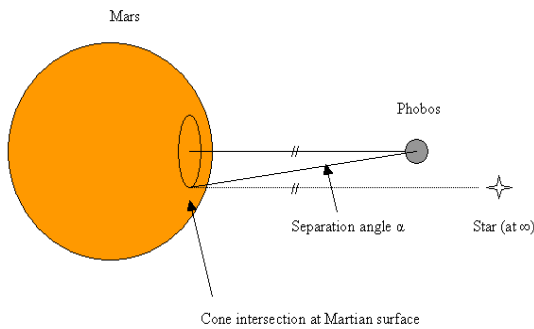

Fig. 2. Celestial Navigation Method for Beagle2

If a second navigation object to target star separation angle measurement is used, the second cone intersection reduces the number of possible lander positions to two. If a third object to star angle measurement is employed, the lander position is uniquely identified.

This method therefore allows determination of the position of a lander with a single image, provided that this image shows a navigation target and 3 stars. If other information sources are available (such as a restriction of the landing area as a result of the entry trajectory design), 2 stars may be sufficient. Obviously, the accuracy of the method will improve if multiple images / multiple targets are available. In that case advanced filters can be employed.

Since the position determination method is based on measurements obtained from processing images, there are a number of factors that contribute to the overall position determination error. The most important error source categories are: Lander and camera hardware (image calibration accuracy and astrometry error, exposure time, S/C clock accuracy), object / imaging geometry (angular separation of target stars, zenith angle), Phobos / Deimos ephemeris data accuracy (σ_{Phobos_at} = 5 km along track, σ_{Phobos_op} = 3 km out of plane, σ_{Phobos_rd} = 3 km radially, from [12]), astrometry (centerfinding error / S/N ratio, number of target stars, navigation target illumination phases), lander target body surface models, and atmospheric conditions (optical depth, geometry).

Assuming an image with 2 stars and Phobos under good geometric conditions, the position of the Beagle2 lander can be determined with an accuracy of ~ 8.25 km (1-σ), based on the performance figures of the Beagle2 SCS camera and the lander clock. Fig. 3 shows the improvement in the position accuracy that can be achieved if a single error source is eliminated. This analysis clearly shows that in the case of Beagle2, the uncertainty in the ephemeris data on Phobos is the main source of error.
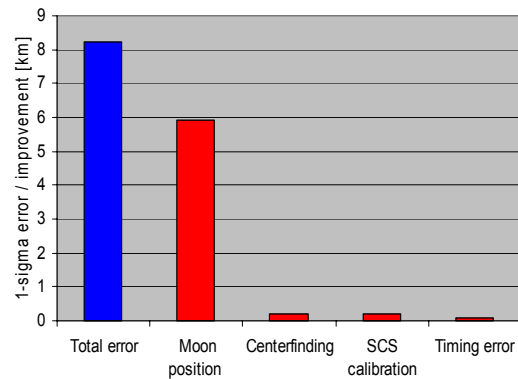

Fig. 3. Position error improvement from elimination of individual error contributions

The proposed celestial navigation method has been verified using NAIF's SPICE system, and a tool for the prediction of suitable imaging opportunity for the Beagle2 lander has been developed. SPICE is a data system designed to assist scientists in planning and interpreting scientific observations from space borne instruments [14]. SPICE consists of data files, also called "kernels" or "kernel files", and a software toolkit whose main component is an extensive subroutine library to read kernel files and produce geometry calculations. This toolkit was used for both the demonstration of the feasibility of the method (a celestial image was simulated based on the assumption of time and lander position, and the corresponding position on the surface of Mars was calculated from where the 'observed' image geometry could be seen) and for the prediction of imaging opportunities for the Beagle2 lander. The B2NAV prediction tool allows to predict favourable image opportunities for the Beagle2 lander, taking into account constraints such as camera FOV, camera filter selection, etc. Fig. 4 illustrates how the different kernels are used to produce the geometry calculations needed to plan a Phobos observation as seen from the nominal position of Beagle2, and to determine its actual position using the astrometry data from SCS images. Required data includes position data of Mars, Phobos, Deimos, and the Sun, orientation data of the Mars body-fixed rotating frame with respect to the J2000 inertial frame, and time correlation data needed to perform conversion between barycentric dynamical time and UTC time. For planning Beagle2 observations, additional kernels containing Beagle2 local-level frame and Beagle2 frame definitions, SCS camera field-of-view parameters, and the Beagle2 nominal position on the Martian surface are employed. Fig. 1 illustrates the calculation of surface intersection coordinates used for the determination of the Beagle2 lander position.

For the actual Beagle2 SCS operations planning and navigation a sophisticated tool will be used, which accurately calculates the overall navigation result and the associated errors as a result of individual error contributions. The verification of this tool will also include star and moon images from previous missions such as Mars Pathfinder.
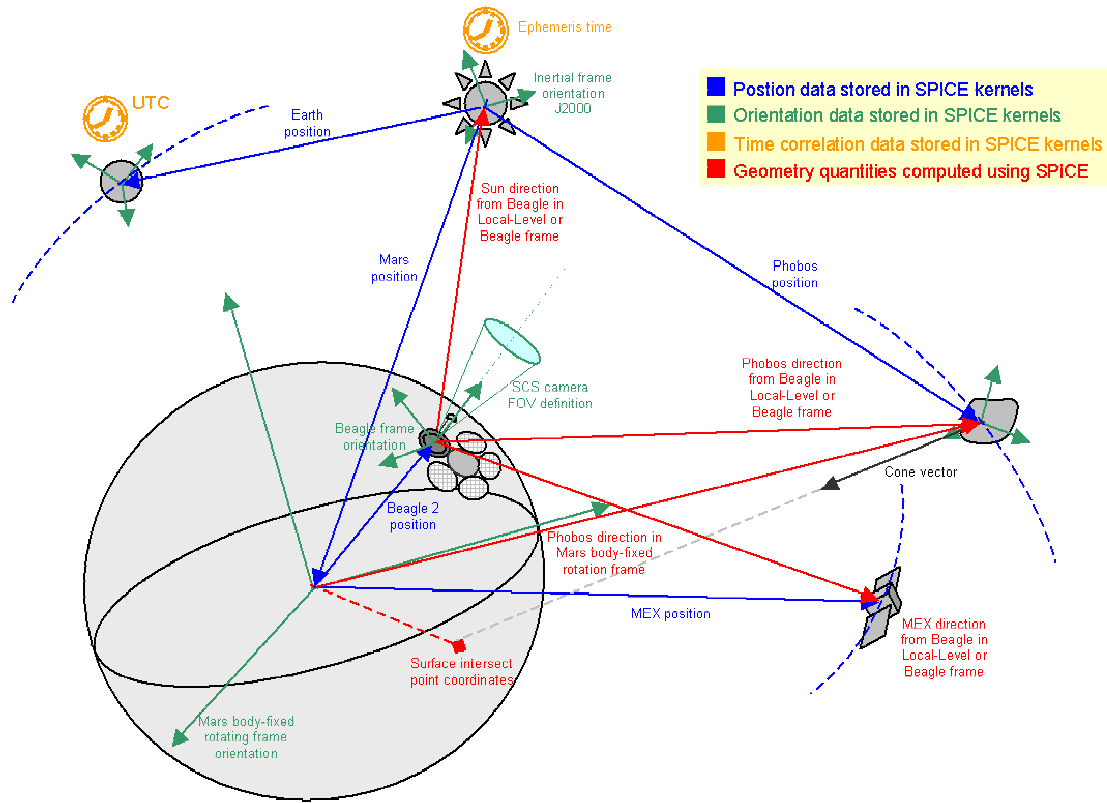

Fig. 4. Reference frames and geometry for celestial navigation calculations with SPICE

4. POSITION DETERMINATION FROM LANDER AND ORBITER IMAGES

In this section we discuss the possibility of using the images returned by the lander for position determination, by attempting to match the configuration of observed terrain features to those seen in existing remotely sensed datasets [15]. The technique was used as long ago as 1966 to find the position of the Surveyor I Moon lander [16] using Earth-based telescope images. Here we particularly consider the use of surface topography data: its appeal is the possibility to directly model what might be seen from the surface. The Mars Global Surveyor MOLA topography dataset [17] is used, and although its resolution is still fairly coarse compared to many of the features that make up a typical landscape view, some MOLA-scale features may be observed. These would provide the most certain reference points, but the most precise measurements are likely to come from lesser features seen only in image data.

Fig. 5 visualizes the Beagle2 landing area based on Mars Global Surveyor MOLA altimetry data with color coding related to the distance from the nominal landing site. Figs. 6 and 7 show simulated panoramas, derived from the MOLA data (gridded at 128 pixels per degree, giving an approximate best resolution of 450m/pixel),

from two points in the vicinity of the nominal landing site at 11.6 N and 90.75 E.
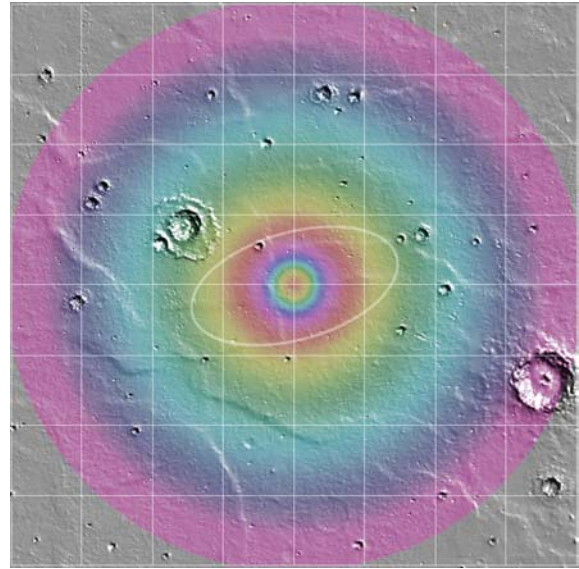

Fig. 5. MOLA shaded relief with radial colour scale and 3-sigma landing ellipse with a grid spacing of 1 degree (57 km).
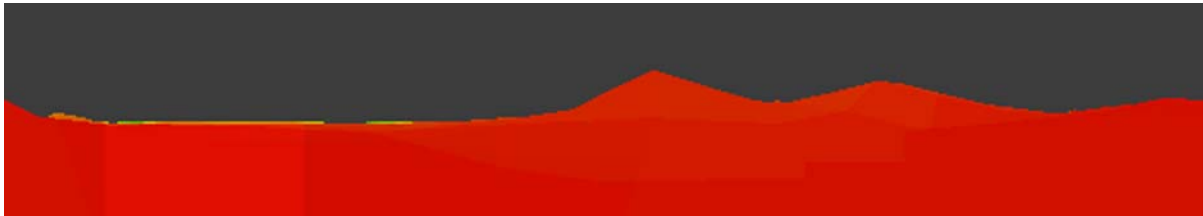

Fig. 6. Simulated panorama from the nominal landing site, 360° view from 15° west of north, clockwise, shown with x20 vertical stretch. Colours correspond to those of Fig. 5. The view from this position is dominated by a 1.2 km crater directly west (2.2 km distant) of the NLS.
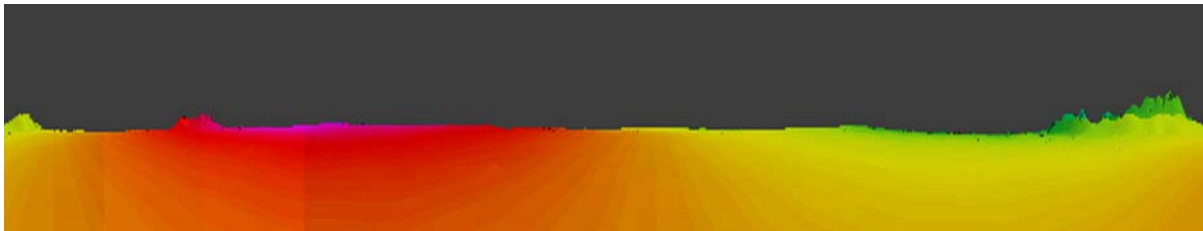

Fig. 7. Simulated panorama from 1 degree west of the nominal landing site. 360° view from 15° west of north, clockwise, shown with x20 vertical stretch. Colours correspond to those of Fig. 5. The red peak is the 5.8 km crater 45 km NW of the nominal landing site; the green / yellow feature is the 25 km crater and its ejecta,

The views give an idea of which local topographic features might be visible to the cameras on the Beagle2, and importantly, from what range they can be seen. Taking account of the planetary curvature, the observation point is placed at a height of ~1m above the interpolated surface; the colour-scale is to assist identification.

The large 25 km crater with a well-defined ejecta blanket to the north-west of the landing site can be observed from 50-85 km distance, the most distant observation being possible from the south-east. This puts it about 30 km too far to be seen from the nominal landing site. The 5.8 km diameter crater situated 45 km north-west of the nominal landing site is on the margin of being observable: according to the model, it can be seen from 40.4 km in this direction. A landing towards this side of the ellipse would likely bring it into view. There are two craters of similar size, 5.3 and 5.8 km, both at around 100 km from the site, one north-east, the other south-east. The northern one can be seen from around 35-40 km, the southern one has somewhat less elevated relief and is seen only from 25-30 km.

The largest crater in the vicinity, of 45 km and to the south-east, is visible from 80-90 km, but being 224 km away, it is unlikely to be observed. Overall, it appears that we are unlikely to see any of the craters of the size range resolvable by MOLA except for that at Lon-0.5 Lat+0.55 relative to the nominal landing site with slightly under 50% probability.

There are 43 craters over 500 m within 57 km (1 deg) of the nominal landing site. The probability of observing one or more of these is of the order of 80%. Within the same range there are about 2500 small knobs which are resolved in THEMIS daytime IR images. The observation of several of these is highly likely. Given an approximate position determined by other means such as celestial navigation, measurements relative to these knobs may determine the lander's position with a precision of tens of metres.

5. APPLICATIONS ON FUTURE MISSIONS

The described combination of celestial navigation and image processing for the position determination of planetary landers offers a number of advantages. There is no payload mass penalty for landers that carry a science camera, and a single image can be sufficient to determine the lander location precisely enough for orbiter image / panorama correlation, coordination of orbiter / lander operations, and mapping of the landing site. Communications payloads can be implemented simpler and lighter because there is no need for a direct link to earth for Doppler tracking in order to support the lander location. The costs for celestial navigation are also expected to be far below the cost of VLBI lander location, which is another ground-based option, but again requires radio contact to Earth. Many planetary bodies in the solar system have natural navigation targets like the Martian Moons. However, any orbiting body – like a relay orbiter such as Mars Express – may serve as a navigation target body, provided that the camera sensitivity is sufficient. For future applications on Mars, an analysis has shown that celestial navigation (using Phobos and Deimos as target bodies) can be performed from ~88% of the Martian surface, assuming a minimum elevation of the navigation targets of 20 deg above the horizon. On Mars, an accuracy of better than 10 km can be expected from a small number of navigation images.

6. CONCLUSIONS

The precise determination of the position of a scientific planetary lander after its touchdown is an important issue for many reasons. Previous Mars landers such as Viking and Mars Pathfinder have used Doppler tracking data for restricting the search area, and a combination of lander panoramas and orbiter images for the detailed determination of the landing sites. In the case of the Viking landers, the results have been ambiguous, and the determination of the lander location on orbiter images depended on the availability of recognizable horizon features. The Beagle2 mission will be the first to use celestial navigation for the coarse determination of the lander position. This can be achieved by taking a single image at an appropriate point in time, and multiple images will improve the results. Assuming an image with 2 stars and Phobos under good geometric conditions, the position of the Beagle2 lander can be determined with an accuracy of ~ 8.25 km (1-σ). The dominant factor for the overall position determination error is the uncertainty in the knowledge of the positions of Phobos and Deimos. The detailed determination of the Beagle2 position will be done by correlation of lander panoramas and high resolution orbiter data. This process will employ data from previous orbiter missions such as Viking, Mars Global Surveyor (MOC, MOLA) and Mars Odyssey (THEMIS), and new data acquired by the Mars Express Orbiter. The celestial navigation method used for Beagle2 allows a position determination at low cost, and without a mass penalty on the lander provided it carries a suitable camera. Potential future application areas are missions to Mars and to other planetary bodies.

7. ACKNOWLEDGEMENTS

8. REFERENCES

1. Morris E. C., Jones K. L. and Berger J. P.,Location of Viking 1 Lander on the Surface of Mars, *ICARUS*, Vol. 34,548-555, 1978.

2. Morris E. C. and Jones K. L., Viking 1 Lander on the Surface of Mars: Revised Location, *ICARUS*, Vol 44, 217-222, 1980.

3. Zeitler W. and Oberst J., The Mars Pathfinder landing Site and the Viking control point network, J.Geophys. Res., Vol 104, No. E4, 8935-8941, 1999.

4. Parker T. J., Kirk R. L. and Davies M. E., Location and Geologic Setting for the Viking 1 lander, LPSC XXX, Abstract No. 2040, Lunar and Planetary Institute, Houston, Texas, March 1999.

5. Zeitler W. and Kuschel M., Where is Viking Lander 2, LPSC XXIX, Abstract No. 1612, Lunar and Planetary Institute, Houston, 2000.

6. Stooke P. J., Locating the Viking 2 Landing Site, LPSC XXIX, Abstract No. 1024, Lunar and Planetary Institute, Houston, 1998.

7. Parker T. J. and Kirk R. L., Location and Geologic Setting of the three US Mars Landers, Fifth International Conference On Mars, Abstract No. 6124, Pasadena, 1999.

8. Griffiths A. D. et al, The Beagle2 Stereo Camera system: Scientific Objectives and Design Characteristics, submitted to Planetary and Space Science, 2003.

9. Griffiths, A. D., Coates, A. J., Josset, J.-L., Paar, G., and Sims, M.R., The Beagle2 Stereo Camera System: Scientific Objectives and Design Characteristics, Geophysical Research Abstracts, Vol. 5, 06365, 2003.

10. Rueffer, P., Borrmann, A., Versatile Image Data Compression For The Beagle 2 Probe, IEEE International Geoscience and Remote Sensing Symposium (IEEE IGARSS 2003), Toulouse, July 2003.

11. Maki, J. N., Lorre, J. J., Smith, P. H., Brandt, R. D. and Steinwand, D. J., The colour of Mars: Spectrophotometric measurements at the Pathfinder landing site, JGR 104, E4, 8788-8794, 1999.

12. MARS, Kieffer et al, The University of Arizona press, Tucson, 1992.

13. Banerdt W. B. and Neumann G. A., The topography (and Ephemeris) of Phobos from MOLA ranging, Abstract. No. 2021, LPSC XXX, 1999.

14. Acton C., SPICE Products Available to the Planetary Science Community. C. H. Acton, LPSC XXX, Abstract No. 1233, Lunar and Planetary Institute, Houston, 1999.

15. Michael, G. G., Beagle2 position determination from the returned camera panoramas using MOLA data. Planetary and Space Science, in press, 2003.

16. Jaffe, L. D. et al., Surveyor I: Preliminary Results. Science 152 (3730), 1737-1750, 1966.

17. Smith, D. and 22 others, Mars Global Surveyor Laser Altimeter Mission Experiment Gridded Data Record, NASA Planetary Data System, MGS-M-MOLA-5-MEGDR-L3-V2.0, 2002.